



# mRNA-Sequencing Analysis Reveals Transcriptional Changes in Root of Maize Seedlings Treated with Two Increasing Concentrations of a New Biostimulant

Sara Trevisan,<sup>\*,†</sup> Alessandro Manoli,<sup>†</sup> Laura Ravazzolo,<sup>†</sup> Clizia Franceschi,<sup>‡</sup> and Silvia Quaggiotti<sup>†</sup>

<sup>†</sup>Department of Agriculture, Food, Natural Resources, Animals and Environment (DAFNAE), University of Padua, Agripolis, Viale dell'Università, 16, 35020 Legnaro, PD, Italy

<sup>‡</sup>ILSA S.p.A., Via Quinta Strada 28, 36071 Arzignano, Italy

## S Supporting Information

**ABSTRACT:** Biostimulants are a wide range of natural or synthetic products containing substances and/or microorganisms that can stimulate plant processes to improve nutrient uptake, nutrient efficiency, tolerance to abiotic stress, and crop quality (<http://www.biostimulants.eu/>, accessed September 27, 2017). The use of biostimulants is proposed as an advanced solution to face the demand for sustainable agriculture by ensuring optimal crop performances and better resilience to environment changes. The proposed approach is to predict and characterize the function of natural compounds as biostimulants. In this research, plant growth assessments and transcriptomic approaches are combined to investigate and understand the specific mode(s) of action of APR, a new product provided by the ILSA group (Arzignano, Vicenza). Maize seedlings (B73) were kept in a climatic chamber and grown in a solid medium to test the effects of two different combinations of the protein hydrolysate APR (A<sub>1</sub> and A<sub>1/2</sub>). Data on root growth evidenced a significant enhancement of the dry weight of both roots and root/shoot ratio in response to APR. Transcriptomic profiles of lateral roots of maize seedlings treated with two increasing concentrations of APR were studied by mRNA-sequencing analysis (RNA-seq). Pairwise comparisons of the RNA-seq data identified a total of 1006 differentially expressed genes between treated and control plants. The two APR concentrations were demonstrated to affect the expression of genes involved in both common and specific pathways. On the basis of the putative function of the isolated differentially expressed genes, APR has been proposed to enhance plant response to adverse environmental conditions.

**KEYWORDS:** RNA-seq, *Zea mays* L., biostimulant, gene expression, root

## INTRODUCTION

Abiotic stresses including drought, temperature extremes, flooding, salinity, and toxic metals strongly compromise crop productivity. Furthermore, the expected global climate changes will enlarge the impact of stresses even further.<sup>1,2</sup> To cope with these concerns, conventional agriculture has been increasing its dependence on chemical fertilizers and pesticides with severe effects on the natural ecosystem and human health.<sup>3</sup> To reorient conventional agriculture toward sustainability, the use survey of nontoxic, natural, active substances is requested together with the assessment of their effectiveness in protection and stimulation of plant performances under suboptimal and even harmful conditions.<sup>4–6</sup> The global market of plant biostimulants has been projected to reach to more than €800 million in 2018 with annual growth potential of 10% or more.<sup>7–9</sup> According to the European Biostimulants Industry Council (EBIC), more than 6 million hectares were annually treated with biostimulant products within European countries, which represents the largest market for this sector.<sup>8</sup> Biostimulants were initially used to promote plant growth in horticulture, where the term biostimulant was apparently coined in 1990s.<sup>10</sup> Nowadays, they are always more frequently used also in conventional crop production to both mitigate environmental impact and enhance crop quality, nutrient efficiency, and abiotic stress tolerance.<sup>11</sup>

In this work, the biostimulant activity of a collagen derived protein thermal hydrolysate, namely APR, developed by ILSA

S.p.A (Arzignano, Vicenza, Italy), on maize seedlings was investigated through both growth and transcriptomic analyses. Protein hydrolysates (HPs) were obtained by chemical, thermal, and/or enzymatic protein hydrolysis from a variety of both vegetal and animal residues.<sup>10,12</sup> HPs have been demonstrated to stimulate nutrient uptake, enhance yield of several horticultural crops, and trigger carbon and nitrogen metabolism by eliciting nitrogen uptake and consequently crop performances.<sup>11,13–20</sup> Several biostimulants have been suggested to have phytohormone-like activities, by hypothesizing that some HPs might both contain precursor of phytohormonal biosynthesis or directly promote auxin- and gibberellin-like effects.<sup>19,21–24</sup> Chelating functions with roles in decreasing plant toxicity to heavy metals and antioxidant activity are also described for some amino acids found as component of HPs.<sup>9,11</sup> Finally, HPs application seems also to stimulate plant tolerance to environmental stresses, including salinity, drought, alkalinity, temperature, and nutrient deficiency.<sup>19,20,25–28</sup> While the knowledge of the benefits of HPs on plants is steadily improving, deeper investigations on molecular mechanisms that regulate beneficial effects of HPs application on plants are needed. In this scenario, deciphering

**Received:** July 6, 2017

**Revised:** October 19, 2017

**Accepted:** October 24, 2017

**Published:** October 24, 2017

the dynamic profiles of the transcriptome in response to APR is central to characterize the mode of action of the newly proposed biostimulant.

RNA-sequencing (RNA-seq) has emerged as a powerful and revolutionary tool to provide high resolution analyses of plant transcriptional dynamics during various aspects of growth and development through sequencing of their associated cDNA (complementary DNA) populations.

Transcriptome analyses of the effects of biostimulants on plants highlighted global changes in gene transcription across multiple processes, pathways, and cell functions.<sup>29–32</sup> However, the knowledge of mechanisms of action of biostimulants under stress or nonstress conditions is still lacking.

In the current study, the effects on growth of two different APR concentrations were assessed in both roots and shoots. Subsequently, RNA-seq analysis was applied on lateral roots to dissect the root transcriptomic profiles in response to the treatments. Gene ontology enrichment analysis of RNA-seq data and KEGG pathway analysis helped in deciphering the complexity of network of metabolic and signaling pathways involved in the regulation of root responses to APR.

To the best of our knowledge, this is the first reported RNA-seq-based study to examine the effect of a solid protein hydrolysate obtained by thermal hydrolysis on maize root transcriptome. These next-generation sequencing data contribute to the available information on the molecular effects exerted by biostimulants on plant roots.

## MATERIALS AND METHODS

**Preparation of Hydrolysates from Tanned Bovine Hides.** APR was obtained by a process of thermobaric hydrolysis applied on trimmings and shavings of bovine hides previously tanned with wet-blue technology. The hydrolysis process was made in spherical rotating autoclaves by high-pressure steam and followed by a low temperature dehydration system.

**Experimental Design and Plant Growth Analyses.** The experiments were carried out on *Zea mays* L. (B73) seedlings. Seeds were germinated on moist paper towels at 25 °C for 72 h. Seedlings were transplanted into vases (16 cm diameter, 20 cm height, volume max 4 L), each containing 3.5 L of river sand. Five days before the transplanting into the pots, 2 different amounts of APR were added in one application with 50 mL of distilled water to the soil mixture: APR high concentration ( $A_1$ ), APR medium concentration ( $A_{1/2}$ ), and a control grown medium (C) (Table 1). The amount of APR, before being distributed in the

**Table 1. Amount of Product Added to 50 mL of Distilled Water**

sample	acronym	amount APR (mg)
APR full dose	$A_1$	23.52
APR half dose	$A_{1/2}$	11.76

vases, was divided into 3 subunits for each concentration and then gradually applied every 5 cm of sand. The amount of APR and the method of its application were first determined in preliminary studies (Ertani, personal communication). Plants were irrigated with 100 mL of a modified Hoagland solution every 2 days according to the following composition ( $\mu\text{M}$ ):  $\text{Ca}(\text{NO}_3)_2$  (200),  $\text{KNO}_3$  (200),  $\text{MgSO}_4$  (200),  $\text{KH}_2\text{PO}_4$  (40),  $\text{FeNaEDTA}$  (10),  $\text{H}_3\text{BO}_3$  (4.6),  $\text{MnCl}_2$  (0.9),  $\text{ZnCl}_2$  (0.09),  $\text{CuCl}_2$  (0.036),  $\text{NaMoO}_4$  (0.01). Plants were placed in a climatic chamber for 15 days; a day/night cycle of 14/10 h at 25/18 °C air temperature, 70/90% relative humidity, and 280  $\mu\text{mol m}^{-2} \text{s}^{-1}$  photon flux density were utilized as standard conditions. A completely random design was used to analyze data. The experiment was carried using three plastic trays each with six vases for each treatment (one plant for each cell). For the plant growth measurements (root and shoot dry weight;

root/shoot ratio), six plants from each plot were chosen for treatment in three independent biological repetitions. For the determination of the dry weight, samples, divided into root and shoot fractions, were transferred in an oven and dried at 80 °C for 72 h. When statistically significant differences were found (ANOVA test), the subsequent test for comparison of treatment means was performed using the Tukey test. Data were analyzed using the program Statistix v. 8.0 (analytical software, Tallahassee, FL, United States).

For the molecular analysis, lateral roots were harvested and subsequently transferred into liquid nitrogen and conserved at  $-80$  °C. Roots from one plant were pooled and represent a single sample out of the three biological replicates (each of six plants). Plants used for sampling roots were excluded from subsequent biomass sampling.

**RNA Isolation and Sequencing Library Preparation.** Three biological replicates were used for all RNA-seq experiments from each treatment. Pooled lateral root tissues were ground in liquid nitrogen, and total RNA was isolated with the TRIzol reagent (Invitrogen, San Giuliano Milanese, Italy). RNA quality was assessed via agarose gel electrophoresis and a Bioanalyzer (Agilent RNA 6000 Nano Chip; Agilent Technologies, Santa Clara, CA, United States). For all samples, an RIN (RNA integrity number)  $\geq 8.0$  was detected.

cDNA libraries for Illumina sequencing were constructed according to the instructions of the manufacturer (TruSeq RNA Sample Preparation; Illumina, San Diego, CA, United States).

**Processing and Mapping of Sequencing Reads.** Base calling was performed using the Illumina Pipeline, and sequences were trimmed with ERNE.<sup>33</sup> Quality trimming removed low quality and ambiguous nucleotides of sequence ends and adapter contamination. TopHat was used to map and annotate the sequences on the B73 reference genome (RefGen\_v2; <ftp://ftp.gramene.org/pub/gramene/maizesequence.org/release-Sb/assembly>, accessed November 7, 2017), and Cufflinks software was used for the analysis of differentially expressed genes (DEGs).<sup>34,35</sup> A single unified assembly from each individual Cufflinks assembly was created thanks to Cuffmerge. Transcripts with a false discovery rate (FDR) of  $\leq 0.05$  were taken as highly significant DEGs.

**Gene Ontology (GO) and Gene Enrichment Analysis.** The PLAZA web tool (<http://bioinformatics.psb.ugent.be/plaza/>) was used to identify GO terms within the different subset of genes.

Data for gene ontology enrichment were computed within PLAZA 2.5 (<http://bioinformatics.psb.ugent.be/plaza/>) for the molecular function, biological processes, and cellular component with default settings.<sup>36,37</sup>

The pathways regulated in the  $A_1$ ,  $A_{1/2}$  and control groups were identified using the Kyoto Encyclopedia of Genes and Genomes (KEGG) database for pathway annotation (<http://www.genome.jp/kegg/>). The pathways that showed the most differentially expressed genes were identified using KEGG mapper ([http://www.genome.jp/kegg/tool/map\\_pathway2.html](http://www.genome.jp/kegg/tool/map_pathway2.html)).

**Hierarchical Clustering.** For each treatment, transcript relative abundance was estimated using the percentage of normalized counts in each fraction relative to the total number of normalized counts. The mean of the relative abundance per fraction was then calculated, and their Euclidean distances computed with the hclust function from the stats R package (R Development Core Team, 2012). Clustering was computed with Ward's minimum variance method and a heat map generated with the gplots R package (2012) (<http://CRAN.R-project.org/package=gplots>).

## RESULTS

**APR Triggers Morphological Responses in Roots.** Biostimulants are assumed to enhance the growth of plants. In this experiment, the biomass production of the maize plants was assessed after 14 days of APR treatments. The effects of two increasing APR doses ( $A_{1/2}$  and  $A_1$ ) on root and shoot dried weight were then evaluated.

For each condition, three biological replicates (RI, RII, and RIII) were analyzed. Replicates were first observed separately (Supporting Information S1). Replicates RII and RIII showed a

statistically significant enhancement of root biomass in the APR-supplied plants, but the differences among the treatments in replicate RI were not significant. No statistically significant differences were obtained from the leaf-biomass analysis, while root/shoot (R/S) ratios, defined as the ratio of below-ground dry biomass (root) to the above-ground dry biomass (stem and leaves), followed the previously observed root biomass behavior.

The subsequent statistical analyses were performed considering all the three replicates (RI, RII, and RIII) per treatment ( $A_1$  and  $A_{1/2}$ ) with respect to the control plants (C) to avoid any misguided interpretation of data. Plants supplemented with APR produced roots with a statistically significant increased biomass (Figure 1). The effect was dose-dependent, with a significantly

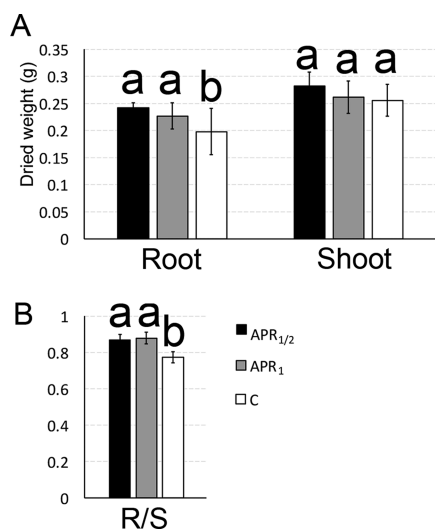


**Figure 1.** Effect of APR application on plant biomass (dried weight, panel A). The distribution of total biomass was reported in panel B. Similar letters at the top of the bars are not significantly different ( $P < 0.05$ ) by an ANOVA-protected LSD test. Each value is plotted as the mean  $\pm$  SE.

greater root biomass (20%) for the half-supplied plants ( $A_{1/2}$ ). A modest but significant effect (12%) on root biomass was

recorded for the plants grown in the presence of the complete dose ( $A_1$ ). Shoot biomass was unchanged in the three growth conditions.

APR treatments resulted in significantly higher mean R/S ratios with no significant difference between the two set of plants ( $A_1$  and  $A_{1/2}$ ). Data indicate that APR preferentially enhanced root rather than shoot growth.

**RNA Sequencing and Mapping of Maize Lateral Root Transcriptome.** To obtain a global view of the transcriptome response of maize to APR, high-throughput RNA sequencing using Illumina sequencing technology was performed on whole RNAs (RNA-seq) extracted from mature root tissues (lateral roots).

RNA sequencing of the 9 samples (2 plant set grown in the presence of different APR doses, namely  $A_1$  and  $A_{1/2}$ , 1 control plant set, and 3 biological replicates) yielded a total of 422.6 million reads, translating to a mean of 47 million reads per sample (Table 2). On average, the RNA-seq experiments yielded between 21 and 62 million reads per sample. Among all reads, 83–90% mapped to unique positions in the maize reference genome. Gene expression levels were quantified and reported as fragments per kilobase of transcript per million mapped reads (FPKM), estimated using Cufflinks.<sup>32</sup>

The expression of 29 332 transcripts (FPKM  $> 1.0$ ) was detected in the mature root (control), whereas APR treated plants had the highest number of expressed genes with 29 441 ( $A_1$ ) and 29 553 ( $A_{1/2}$ ) expressed genes.

**Global Transcriptome Changes after Plant Treatment with APR and Hierarchical Cluster Analysis.** To reveal the transcriptome changes influenced by APR, DEGs were identified by pairwise comparison of samples collected ( $A_{1/2}$  vs C;  $A_1$  vs C;  $A_1$  vs  $A_{1/2}$ ). Cuffdiff analysis revealed 1006 DEGs, among which only 2.8% (29 DEGs) were shared by all comparison groups (Figure 2).

When FDR was controlled at 5%, 290 and 643 genes were differentially expressed in response to the half-dose of APR and whole concentration, respectively (Figure 2). Complete lists of differentially expressed genes treated with both the doses are shown in Supplementary Table S1.

**Table 2. Overview of Mapping of RNA-Seq Reads against the Reference Genome**

	no. of total reads	no. of mapped reads	unique	multimatch	no. of reads not mapped
C I	24 533 666	23 706 845	7 433 476	13 366 106	3 734 084
	100%	85%	30%	54%	15%
C II	21 577 159	20 846 219	6 631 057	11 791 340	3 154 762
	100%	85%	30%	54%	14%
C III	53 162 801	50 042 447	15 806 066	27 270 460	10 086 275
	100%	81%	30%	51%	19%
$A_{1/2}$ I	53 240 810	51 373 724	16 399 119	29 083 434	7 758 257
	100%	85%	31%	55%	15%
$A_{1/2}$ II	51 991 656	48 916 524	15 688 547	27 079 132	9 223 977
	100%	82%	30%	52%	18%
$A_{1/2}$ III	61 877 965	58 783 574	18 558 753	32 917 386	10 401 826
	100%	83%	30%	53%	17%
$A_1$ I	62 321 113	60 344 872	19 105 436	33 865 304	9 350 373
	100%	85%	31%	54%	15%
$A_1$ II	30 729 395	29 686 021	9 409 630	16 657 808	4 661 957
	100%	85%	31%	54%	15%
$A_1$ III	63 235 017	60 726 828	19 421 068	34 165 344	9 648 605
	100%	85%	31%	54%	15%

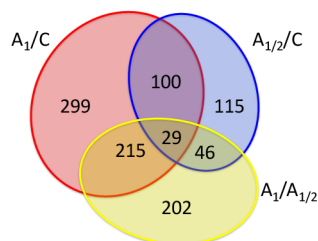


**Figure 2.** Venn diagrams showing the comparison in gene expression in lateral root of maize seedlings treated with two increasing APR concentration ( $A_{1/2}$  and  $A_1$ ). In the graphic, the comparison between the concentrations respect to the control ( $A_{1/2}/C$  and  $A_1/C$ ) and respect to each other ( $A_1/A_{1/2}$ ) is reported (change,  $\geq 1.5$ -fold;  $p \leq 0.005$ ). Nonoverlapping numbers represent the number of genes unique to a treatment. Overlapping numbers represent the number of mutual genes between treatments.

When the genes differentially regulated by the highest APR concentration with respect to the control are considered, 643 DEGs were almost equally divided as up-regulated (329 DEGs) and down-regulated (314 DEGs) (Figure 2 and Figure 3).

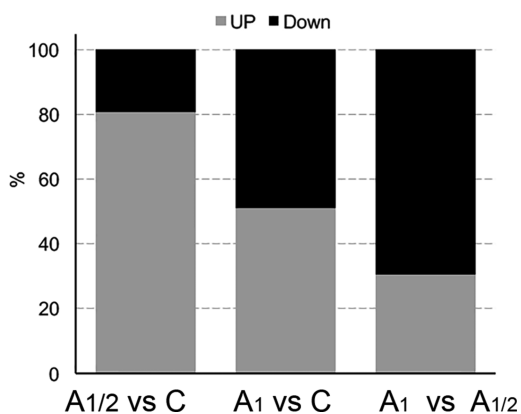


**Figure 3.** Diagram representing the percent of genes differentially expressed in each comparison ( $A_{1/2}/C$ ,  $A_1/C$ ,  $A_1/A_{1/2}$ ). Only DEGs with FDR  $< 5\%$  were included. DEGs were classified as up-regulated or down-regulated (comparison between the treatments is  $>1$  or  $<1$ , respectively) according to their RPKM values.

The number of DEGs isolated in the comparison between the highest concentration versus the control was markedly higher than the number of differentially expressed genes detected by the half-dose experiment (290 DEGs), suggesting a greater impact of the higher APR dose on root transcriptome. It is noteworthy that the half dose resulted in the up-regulation of the 80.7% of the DEGs identified (Figure 3).

Both the applications ( $A_1$  and  $A_{1/2}$ ) affect gene expression, regulating the transcription of a consistent part of them (48 and 54% respectively) to a small degree (fold change  $>0.5$  or  $<2$ ).

A stronger effect (fold change  $\geq 2$  or  $\leq 0.5$ ) is evident on the remaining transcripts (52 and 46% for  $A_1$  and  $A_{1/2}$ , respectively) (Figures 4 and 5). Further examination of the results showed that 129 DEGs were coregulated by the two applications, with most of them (96%) showing the same (i.e., increased or decreased relative expression) in both the theses. Only four of them (GRMZM2G037454, GRMZM2G026930, GRMZM5G833699, and GRMZM2G063287) were found to have a conflicting pattern of expression.

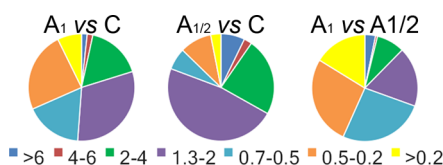


**Figure 4.** Fold changes distribution of DEGs identified by the RNaseq experiments in the three comparisons analyzed. The ratios reported represents two APR treatments ( $A_1$ ,  $A_{1/2}$ ) and control (C).

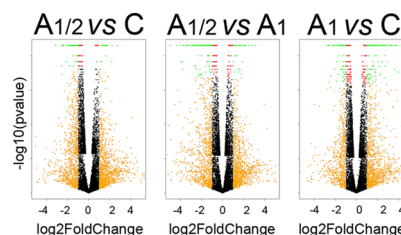


**Figure 5.** Volcano plot of changes in gene expression for  $A_{1/2}$ -treated and  $A_1$ -treated maize plants relative to control.  $M$  versus  $U$  is reported in panel C. Plotted are the  $p$ -values on the  $y$ -axes in log 10 scale against the ratio of gene expression on the  $x$ -axes in log 2 scale. The cutoff criteria (change,  $\geq 2$ -fold;  $p \leq 0.005$ ) are indicated.

A total of 514 genes was differentially exclusively regulated by  $A_1$  concentration, while 161 DEGs were unique to  $A_{1/2}$  concentration (Figure 2).

The comparison between the two APR treatments ( $A_1$  vs  $A_{1/2}$ ) identified 492 transcripts with significant different expression values with 207 of them showing a conserved expression pattern (94 DEGs increased and 113 DEGs decreased relative expression respect to control sample), thus suggesting a dose effect for the studied product. A discrepancy in expression profiles was instead recorded for 87 DEGs ( $A_1 > C$ ,  $A_{1/2} < C$ ) and for 198 DEGs ( $A_{1/2} > C$ ,  $A_1 < C$ ). For these genes, the transcript accumulation did not correlate with the amount of product provided to the plants, and the half-dose treatment was the most effective in regulating transcriptional activity.

The most responsive genes to both concentrations of APR (FC  $> 10$  or FC  $< 0.1$ ) are listed in Table 3.

Among the DEGs with the highest FC (in comparison with control), a brassinosteroid LRR receptor kinase (GRMZM2G172330), a putative Zn-dependent exopeptidases superfamily protein (GRMZM2G324703), a calcium-dependent protein kinase (GRMZM2G332660), an alkenal reductase (NADP(+)-dependent (GRMZM2G125196), and an epiaristolochene 1,3-dihydroxylase (GRMZM2G154828) were identified. Also, a high expression level for six genes (GRMZM2G-704488, GRMZM2G030036, AC233955.1\_FG003, GRMZM2G124785, GRMZM2G385200, and GRMZM2G156599) involved in nicotianamine biosynthesis was detected in the APR-treated sample (Table 3 and Supporting Information S2).

A hierarchical cluster analysis was performed on the 1006 DEGs to investigate the gene expression profiles in the three samples. Hierarchical clustering generated six groups of transcripts sharing similar expression profiles (Figure 6).

**Functional Annotation and Classification of Maize Lateral Root Transcriptome.** To investigate the biological function of DEGs in response to APR, GO analysis and assessment of enrichment of all detected annotated transcripts grouped for treatments were executed using PLAZA monocots platform ([http://bioinformatics.psb.ugent.be/plaza/versions/plaza\\_v3\\_monocots/](http://bioinformatics.psb.ugent.be/plaza/versions/plaza_v3_monocots/)).

Table 3. List of the Most Responsive Genes for Each APR Concentration

	gene ID	description	gene ID	description			
FC > 3.5	GRMZM5G808876	$A_{1/2}$ adenylate kinase	FC > 3.5	GRMZM2G172330 $A_1$ brassinosteroid insensitive 1-associated receptor kinase 1			
	GRMZM2G072383	uncharacterized protein		GRMZM2G324703	Zn-dependent exopeptidases superfamily protein		
	GRMZM2G072322	abundant protein 76		GRMZM2G176081	uncharacterized protein		
	GRMZM2G044627	OBAP1A; oil body-associated protein 1A		GRMZM2G332660	calcium-dependent protein kinase		
	GRMZM2G324703	Zn-dependent exopeptidases superfamily protein		GRMZM2G702888	protein coding		
	GRMZM2G085381	benzoxazinless1; indole-3-glycerol phosphate lyase		GRMZM2G082830	inactive L-type lectin-domain containing receptor kinase III.1		
	GRMZM2G417905	putative ubiquitin-like-specific protease 1B		GRMZM2G125196	alkenal reductase (NADP (+)-dependent		
	GRMZM2G437711	SNF2 protein		GRMZM2G037284	Golgi organization protein 2 homologue		
	GRMZM2G140293	uncharacterized protein		GRMZM2G049852	toxin extrusion protein 1		
	GRMZM2G156079	pebp2: phosphatidylethanolamine-binding protein2		GRMZM2G154828	epiaristolochene 1,3-dihydroxylase		
	GRMZM2G125196	alkenal reductase (NADP (+)-dependent		GRMZM2G421126	UDP-D-xylose:L-fucose $\alpha$ -1,3-D-xylosyltransferase		
	GRMZM2G138752	epiaristolochene 1,3-dihydroxylase		GRMZM2G703293	serine carboxypeptidase-like		
	GRMZM2G179143	putative laccase-19		GRMZM2G425993	uncharacterized protein		
	AC234190.1_FG002	crocetin glucosyltransferase 2, indole-3-acetate $\beta$ -glucosyltransferase		GRMZM2G437711	SNF2 protein		
	FC < 0.4	GRMZM2G354909		carbonyl reductase [NADPH] 1	FC < 0.1	GRMZM2G174192	anthocyanidin 3-O-glucosyltransferase
		GRMZM2G096683		polyol transporter		GRMZM2G16265	embryo specific protein 5
		AC218998.2_FG011		(13E)- $\lambda$ -7,13-dien-15-ol synthase		GRMZM2G045720	eukaryotic peptide chain release factor subunit 1
GRMZM2G000423		flavonol synthase/flavanone 3-hydroxylase	GRMZM2G428040	transcription activator-related			
GRMZM2G112539		xyloglucan endotransglucosylase/hydrolase	GRMZM2G354909	carbonyl reductase [NADPH] 1			
GRMZM2G117989		Win1, pathogenesis-related protein PR	GRMZM2G079440	dehydrin DHN1			
GRMZM2G106393		uncharacterized protein	GRMZM2G061303	nitrate transporter 1.5			
GRMZM2G061303		nitrate transporter 1.5	GRMZM2G412436	embryonic protein DC-8			
GRMZM5G812170		uncharacterized protein	GRMZM2G023520	uncharacterized protein			
GRMZM2G046163		tryptophan synthase $\alpha$ -chain	GRMZM2G122654	Amorpha-4,11-diene 12-monooxygenase			
GRMZM2G124921		patatin group M, patatin T5	GRMZM2G407223	uncharacterized protein			
GRMZM2G446454	epi-6-deoxocathasterone 23-monooxygenase	AC206425.3_FG002	jasmionate-induced protein				
GRMZM2G023520	uncharacterized protein						

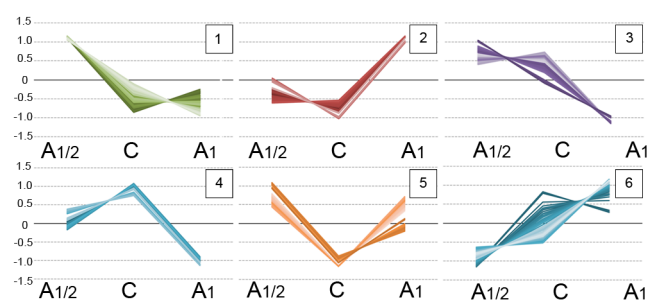


**Figure 6.** Clustering results of data from RNA-seq by STEM analysis. Each box corresponds to a model expression profile in response to APR. The number in the top right-hand corner of a profile box is the cluster number.

The analysis of the 284 up-regulated DEGs identified in the  $A_1$  vs C comparison resulted in the assignment of 1997 unique GO functional annotation terms (Figure 7). Of them, 1304 annotations were within the biological process category, accounting for up to 70% of the total GO functional annotation categories, and the rest were within the cellular component (166 annotations) and molecular function categories (526 annotations).

In the biological process classification, the most frequent GO accessions were response to stimulus, oxidation-reduction process, localization, and transport. Genes involved in ion binding and oxidoreductase activity were the most prominent molecular function accession occurring in maize lateral root transcriptome after  $A_1$  treatment. The genes with a significant down-regulation of the expression levels after APR provision ( $A_1$ ) include terms such as response to stimulus, biosynthetic processes, response to stress, and response to abiotic stimulus.

The 234 up-regulated genes by the lowest dose ( $A_{1/2}$ ) provision lead to the identification of 1041 GO annotations, while the 56 down-regulated transcripts resulted in 488 terms.

The most frequent annotations (biological processes) were oxidation-reduction process, response to stimulus, organic cyclic compound metabolic process, establishment of localization, and transport. Molecular function category (Supporting Information S4) includes stress-related terms such as ion binding, oxidoreductase activity, transferase activity, and cation binding for both up- and down-regulated transcripts.

For KEGG (Kyoto Encyclopedia of Genes and Genomes, <http://www.kegg.jp/>) analysis, a total of 220 ( $A_{1/2}$  vs C) and 502 ( $A_1$  vs C) DEGs were mapped to identify active pathways in *Zea mays* L.

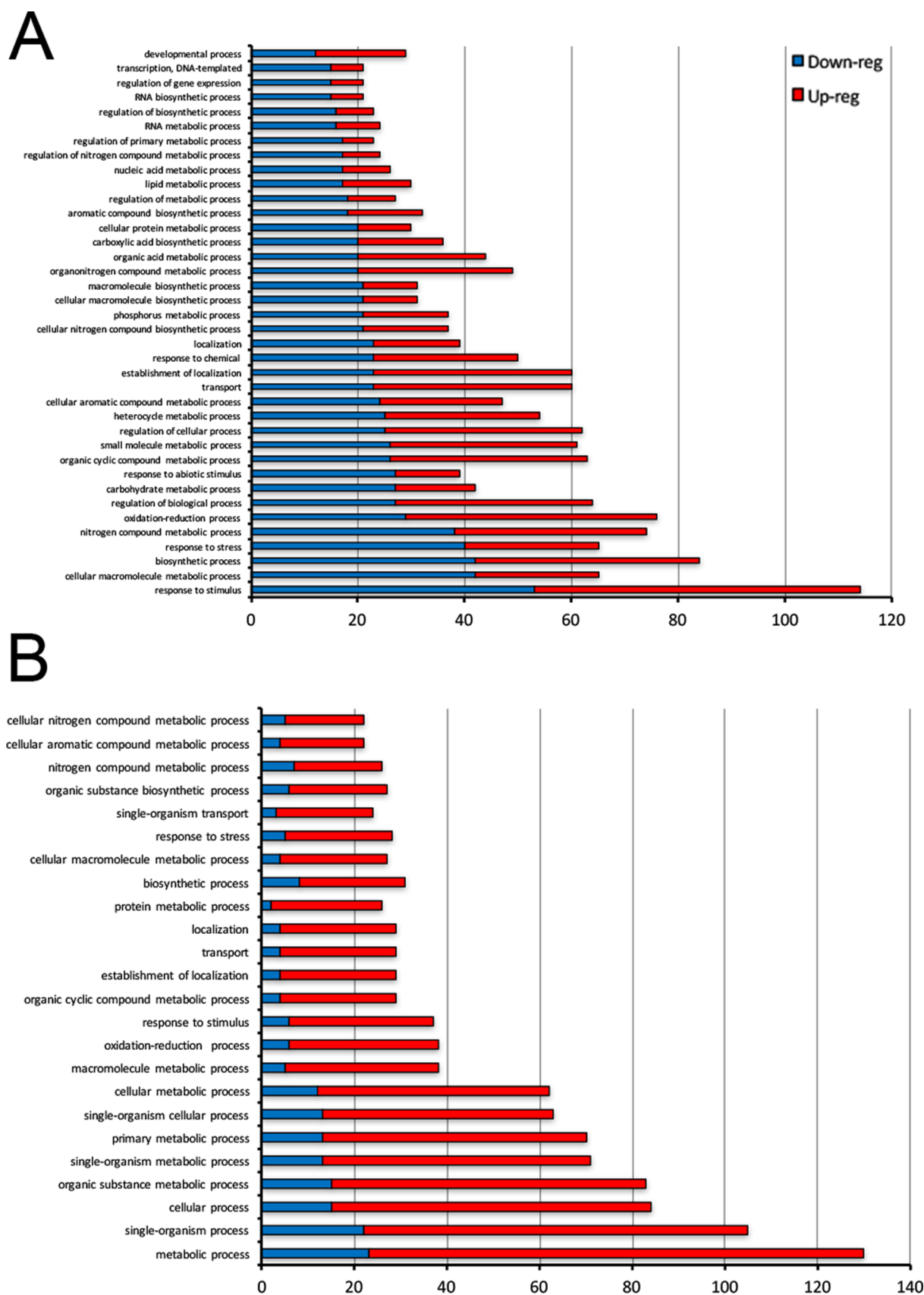


**Figure 7.** Overview of the GO classification of the 1006 DEGs identified by the RNA seq analysis on mature root of maize seedlings grown in presence or absence of APR. The most numerous GO terms identified in the comparison  $A_1$  vs C are reported in the panel A. The GO terms related to  $A_{1/2}$  vs C comparison are reported in Panel B.

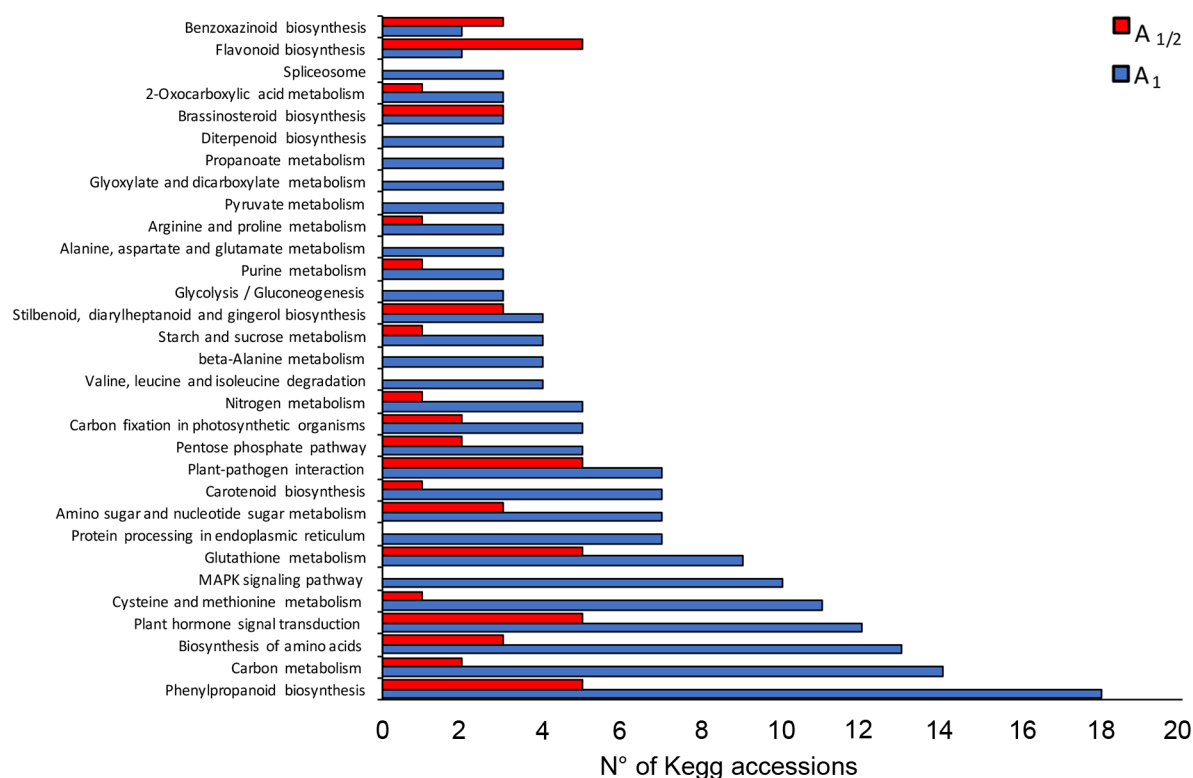


**Figure 8.** Overview of the KEGG annotation of all DEGs identified by the RNA seq analysis on mature root of maize seedlings grown in the presence or absence of APR. The most numerous KEGG terms identified in the comparisons are reported.

In total, 72 pathways were identified using the DEGs isolated in the two comparisons as query (Figure 8). The largest category was metabolic pathways (Supporting Information S8), followed by biosynthesis of secondary metabolites, phenylpropanoid biosynthesis, carbon metabolism, biosynthesis of amino acids, plant hormone signal transduction, MAPK signaling pathway, and glutathione metabolism. These annotations provide a further understanding of the transcriptome data and their functions and pathways in *Zea mays* L.

**GO Enrichment of the Maize Lateral Root Transcriptome after APR Applications.** The GO terms connected to the genes herein identified were analyzed to obtain useful information about the transcriptome response to APR treatments.

GO term enrichment analysis of the APR-upregulated transcripts (A<sub>1</sub> and A<sub>1/2</sub>) indicated various biological processes and molecular functions involved in abiotic stress response such as response to oxidative stress, iron ion transport, oxidation–reduction process, and nicotianamine synthase activity (Figure 9).

Intragroup analysis (Figure 9) revealed that in the comparisons of A<sub>1/2</sub> and A<sub>1</sub> vs control, the top significantly enriched GO functional annotation categories among the up-regulated genes were response to oxidative stress, iron ion transport, and nicotianamine biosynthetic process and DNA binding.

The significantly enriched GO functional annotation categories among the down-regulated DEGs in response to A<sub>1/2</sub> supply were mainly related to abiotic stress response: response to water, response to cold (biological process), sucrose synthase activity, and iron ion binding (molecular function). The highest concentration (A<sub>1</sub>) resulted in the down-regulation of DEGs enriched in response to stress, response to abiotic stimulus,

response to stimulus, response to high light intensity, carbohydrate metabolic process, response to temperature stimulus, hydrolase activity, protein binding, and zinc ion binding.

To better investigate the correlation between the dose of the product and the alteration in gene expression, a GO term enrichment analysis was performed for each of the previously identified clusters (Figure 9). The analysis demonstrates that all six clusters present GO terms associated with stress.

In the biological process category, GO terms related to stress response (oxidation–reduction process, cellular response to nitric oxide, toxin metabolic process, and regulation of brassinosteroid biosynthetic process) were present in clusters grouping up-regulated transcripts (1, 2, and 5; Table 4). Cluster 6 shows a negative effect of APR for gene expression and presents enrichment GO terms involved in cell growth such as actin filament organization, cytoskeleton organization, plant-type cell wall modification, and carbohydrate metabolic process (Table 4). Go-enriched terms of cluster of genes in which expression is altered in opposite direction by the two APR doses (cluster 3) are oxidoreductase activity, response to abiotic stimulus, and cell wall organization. Cluster 4 presents an enriched hydrolase activity among the GO terms of molecular functions category (Table 4). Interestingly GO terms related to oxidoreductase activity are present in the list of annotations concerning molecular function of each cluster except for cluster six, which is enriched only for the actin binding term (Table 5).

**Manual Classification of DEGs.** Gene ontology analysis revealed a strong presence of transcripts involved in stress response. Their annotations were manually grouped according to their biological functions. In the following section, a brief overview of the different groups was reported.

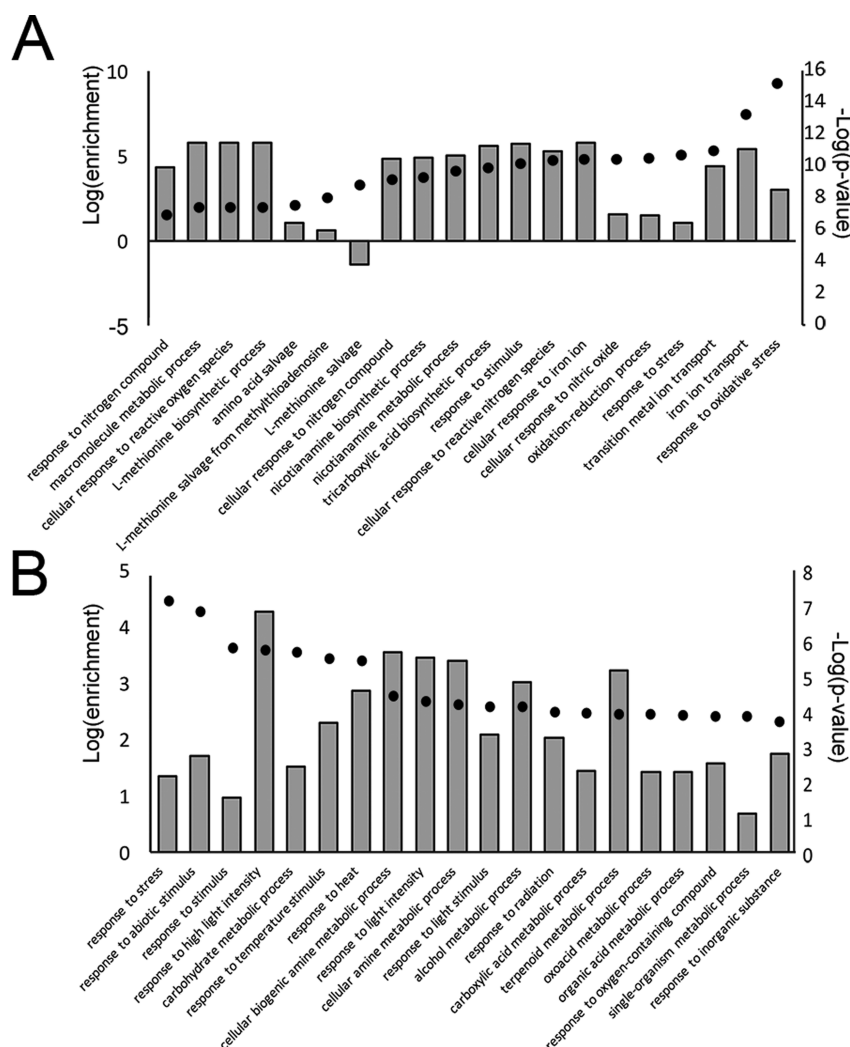


**Figure 9.** Enrichment analysis of DEGs identified by the RNaseq analysis on mature root of maize seedlings grown in presence or absence of the new biostimulant APR. The most significant terms identified in the comparison A<sub>1</sub> vs C are reported in panel A. Panel B contains only the enriched terms related to A<sub>1/2</sub> vs C comparison.

The largest group of transcripts that were dysregulated by the supply of two different doses of APR is the transporters group (Supporting Information S3). Transporters for nitrate, nitrite, phosphate, potassium, amino acid, heavy metals (iron, zinc, and copper), aquaporins, and toxin extrusion proteins were included in this group. Moreover, six of the nine maize genes coding for nicotianamine synthase (ZmNAS) were identified and included in this group (Supporting Information S2).

The expression levels of 5 of these genes (GRMZM2G385200, GRMZM2G156599, AC233955.1\_FG003, GRMZM2G704488, GRMZM2G030036, and GRMZM2G124785) were significantly upregulated (2.5-fold) by APR applications with respect to the control with a stronger effect of the highest concentration (A<sub>1</sub>). Only one transcript (GRMZM2G478568, ZmNAS3) was down-regulated by both the APR applications.

Previous studies have shown that transcription factors (TFs) can affect the plant response to abiotic stress. In total, 32 differentially expressed genes belonging to several TFs families were identified herein (Supporting Information S4), namely WRKY, ethylene-responsive factors (ERF), basic leucine zipper (bZIP), LOB domain, and myeloblastosis protein (MYB) families. The four most abundant TF groups were AP2/EREBP, WRKY, and bHLH.

A significant transcriptional regulation for several genes encoding proteins with antioxidant activity, including a large set of peroxidases (28), laccase (5), and glutathione-S-transferase (8), was also detected (Supporting Information S5). The APR supply resulted in a general induction of their transcription but with dose-dependent effects. In some cases, the effect was greater in the sample provided with the half dose (A<sub>1/2</sub>) (AC210003.2\_FG004, AC205413.4\_FG001, GRMZM2G400390, GRMZM5G800488, GRMZM2G320786, GRMZM2G305526, AC234190.1\_FG002, GRMZM2G156877, GRMZM2G146246, and GRMZM2G302373), straightening the hypothesis of a dose-dependent effect of the product. An interesting expression profile was recorded for the laccase AC234190.1\_FG002, which showed up to 3.5-fold increase in expression in response to A<sub>1/2</sub> application. The A<sub>1</sub> application did not induce any change in the AC234190.1\_FG002 transcript accumulation with respect to the control.

Furthermore, the half-APR supply (A<sub>1/2</sub>) resulted in a down regulation of 9 Hsp, two DnaJ proteins, and three DnaK proteins (Supporting Information S6).

Some DEGs involved in hormonal pathways were also identified in this study. RNaseq analysis identified the differential expression of 10 brassinosteroid insensitive 1-associated receptor



Table 4. GO Enrichment Analysis of the Six Clusters Identified<sup>a</sup>

cluster	N <sup>o</sup> of DEG	GO term	log 2 enrichment	p-value	description
1	145	GO:0055114	1.78	$7.56 \times 10^{-6}$	oxidation–reduction process
		GO:0006979	2.92	$2.90 \times 10^{-5}$	response to oxidative stress
		GO:0043086	4.28	$1.58 \times 10^{-4}$	negative regulation of catalytic activity
		GO:0044092	4.05	$2.92 \times 10^{-4}$	negative regulation of molecular function
		GO:0006950	1.42	$8.57 \times 10^{-4}$	response to stress
2	248	GO:0046688	6.24	$9.04 \times 10^{-4}$	response to copper ion
		GO:0006979	3.26	$4.62 \times 10^{-15}$	response to oxidative stress
		GO:0006826	5.7	$1.85 \times 10^{-13}$	iron ion transport
		GO:0071281	5.76	$3.22 \times 10^{-12}$	cellular response to iron ion
		GO:0071732	6.29	$3.85 \times 10^{-12}$	cellular response to nitric oxide
		GO:0071731	6.19	$7.18 \times 10^{-12}$	response to nitric oxide
		GO:0000041	4.75	$1.04 \times 10^{-11}$	transition-metal ion transport
		GO:1902170	6.09	$1.27 \times 10^{-11}$	cellular response to reactive nitrogen species
		GO:0071248	5.53	$1.42 \times 10^{-11}$	cellular response to metal ion
		GO:0071241	5.38	$3.68 \times 10^{-11}$	cellular response to inorganic substance
		GO:0044710	1.17	$4.41 \times 10^{-11}$	single-organism metabolic process
		GO:0010039	5.33	$4.93 \times 10^{-11}$	response to iron ion
		GO:0006950	1.67	$1.65 \times 10^{-10}$	response to stress
		GO:0055114	1.7	$3.57 \times 10^{-10}$	oxidation–reduction process
		GO:0072351	6.29	$7.45 \times 10^{-9}$	tricarboxylic acid biosynthetic process
		GO:0030417	6.29	$7.45 \times 10^{-9}$	nicotianamine metabolic process
		GO:0030418	6.29	$7.45 \times 10^{-9}$	nicotianamine biosynthetic process
		GO:1901698	3.78	$9.67 \times 10^{-9}$	response to nitrogen compound
		GO:0044699	0.73	$9.75 \times 10^{-9}$	single-organism process
		GO:1901699	4.85	$1.22 \times 10^{-8}$	cellular response to nitrogen compound
		GO:0034614	4.81	$1.48 \times 10^{-8}$	cellular response to reactive oxygen species
		GO:0050896	1.21	$1.79 \times 10^{-8}$	response to stimulus
		GO:0071267	6.02	$2.31 \times 10^{-8}$	L-methionine salvage
		GO:0019509	6.02	$2.31 \times 10^{-8}$	L-methionine salvage from methylthioadenosine
		GO:0043102	6.02	$2.31 \times 10^{-8}$	amino acid salvage
		GO:0071369	4.7	$2.55 \times 10^{-8}$	cellular response to ethylene stimulus
		GO:0034599	4.63	$3.57 \times 10^{-8}$	cellular response to oxidative stress
		GO:0071265	5.91	$3.73 \times 10^{-8}$	L-methionine biosynthetic process
		GO:0010038	2.95	$4.24 \times 10^{-8}$	response to metal ion
		GO:0009723	4.02	$9.92 \times 10^{-8}$	response to ethylene
		GO:1901564	1.7	$1.54 \times 10^{-7}$	organonitrogen compound metabolic process
		GO:0072350	5.52	$1.75 \times 10^{-7}$	tricarboxylic acid metabolic process
GO:0044281	1.53	$3.24 \times 10^{-7}$	small molecule metabolic process		
GO:0010233	6.29	$3.33 \times 10^{-7}$	phloem transport		
GO:0010232	6.29	$3.33 \times 10^{-7}$	vascular transport		
GO:0044711	1.63	$6.44 \times 10^{-7}$	single-organism biosynthetic process		
GO:0043094	3.94	$1.05 \times 10^{-6}$	cellular metabolic compound salvage		
GO:0009086	5.02	$1.15 \times 10^{-6}$	methionine biosynthetic process		
GO:1901566	2.09	$1.45 \times 10^{-6}$	organonitrogen compound biosynthetic process		
GO:0044272	3.52	$1.47 \times 10^{-6}$	sulfur compound biosynthetic process		
GO:0016053	2.27	$1.55 \times 10^{-6}$	organic acid biosynthetic process		
GO:0046394	2.27	$1.55 \times 10^{-6}$	carboxylic acid biosynthetic process		
GO:0010035	2.2	$2.73 \times 10^{-6}$	response to inorganic substance		
GO:0019752	1.8	$3.18 \times 10^{-6}$	carboxylic acid metabolic process		
GO:0044283	2.08	$3.28 \times 10^{-6}$	small molecule biosynthetic process		
GO:0043436	1.79	$3.51 \times 10^{-6}$	oxoacid metabolic process		
GO:0006082	1.79	$3.57 \times 10^{-6}$	organic acid metabolic process		
GO:0006555	4.65	$4.40 \times 10^{-6}$	methionine metabolic process		
GO:0015684	6.55	$7.65 \times 10^{-6}$	ferrous iron transport		
GO:0000302	3.44	$1.13 \times 10^{-5}$	response to reactive oxygen species		
GO:0043170	−1.02	$1.15 \times 10^{-5}$	macromolecule metabolic process		
GO:0044260	−1.12	$1.25 \times 10^{-5}$	cellular macromolecule metabolic process		
GO:0042401	4.25	$1.82 \times 10^{-5}$	cellular biogenic amine biosynthetic process		
GO:0009309	4.25	$1.82 \times 10^{-5}$	amine biosynthetic process		
GO:0006790	2.96	$2.64 \times 10^{-5}$	sulfur compound metabolic process		
GO:0000097	4.09	$3.24 \times 10^{-5}$	sulfur amino acid biosynthetic process		

Table 4. continued

cluster	N <sup>o</sup> of DEG	GO term	log 2 enrichment	p-value	description
		GO:0030001	2.34	$3.29 \times 10^{-5}$	metal ion transport
		GO:0009067	4.05	$3.60 \times 10^{-5}$	aspartate family amino acid biosynthetic process
		GO:0006811	1.72	$7.08 \times 10^{-5}$	ion transport
		GO:0009066	3.78	$9.23 \times 10^{-5}$	aspartate family amino acid metabolic process
		GO:0044267	-1.71	$9.39 \times 10^{-5}$	cellular protein metabolic process
		GO:0042221	1.4	$9.78 \times 10^{-5}$	response to chemical
		GO:0006520	1.91	$1.12 \times 10^{-4}$	cellular amino acid metabolic process
		GO:0008652	2.42	$1.34 \times 10^{-4}$	cellular amino acid biosynthetic process
		GO:0000096	3.63	$1.49 \times 10^{-4}$	sulfur amino acid metabolic process
		GO:0006576	3.63	$1.49 \times 10^{-4}$	cellular biogenic amine metabolic process
		GO:0019538	-1.33	$2.16 \times 10^{-4}$	protein metabolic process
		GO:0044106	3.48	$2.46 \times 10^{-4}$	cellular amine metabolic process
		GO:0006098	4.08	$2.62 \times 10^{-4}$	pentose-phosphate shunt
		GO:0055076	4.08	$2.62 \times 10^{-4}$	transition-metal ion homeostasis
		GO:0006740	4.04	$2.91 \times 10^{-4}$	NADPH regeneration
		GO:0015675	6.7	$3.65 \times 10^{-4}$	nickel cation transport
		GO:0009308	2.93	$3.89 \times 10^{-4}$	amine metabolic process
		GO:1901607	2.59	$4.49 \times 10^{-4}$	$\alpha$ -amino acid biosynthetic process
		GO:0006739	3.83	$5.15 \times 10^{-4}$	NADP metabolic process
		GO:0006812	1.76	$5.58 \times 10^{-4}$	cation transport
		GO:0072511	3.2	$6.07 \times 10^{-4}$	divalent inorganic cation transport
		GO:0044763	0.57	$6.75 \times 10^{-4}$	single-organism cellular process
		GO:0008152	0.34	$6.80 \times 10^{-4}$	metabolic process
		GO:0051704	1.7	$7.82 \times 10^{-4}$	multiorganism process
		GO:0055072	4.48	$9.19 \times 10^{-4}$	iron ion homeostasis
		GO:0044765	1.05	$9.72 \times 10^{-4}$	single-organism transport
3	139	GO:0055114	1.65	$9.28 \times 10^{-6}$	oxidation–reduction process
		GO:0009628	1.74	$5.66 \times 10^{-4}$	response to abiotic stimulus
4	231	GO:0009685	5.51	$9.98 \times 10^{-5}$	gibberellin metabolic process
		GO:0006576	3.73	$1.09 \times 10^{-4}$	cellular biogenic amine metabolic process
		GO:0006950	1.18	$1.35 \times 10^{-4}$	response to stress
		GO:0044106	3.57	$1.81 \times 10^{-4}$	cellular amine metabolic process
		GO:0050896	0.9	$1.84 \times 10^{-4}$	response to stimulus
		GO:0046173	5.16	$2.16 \times 10^{-4}$	polyol biosynthetic process
		GO:0009644	4.13	$2.26 \times 10^{-4}$	response to high light intensity
		GO:0016101	4.88	$3.97 \times 10^{-4}$	diterpenoid metabolic process
		GO:0009266	2.1	$6.54 \times 10^{-4}$	response to temperature stimulus
		GO:0019752	1.48	$7.29 \times 10^{-4}$	carboxylic acid metabolic process
		GO:0009628	1.41	$7.74 \times 10^{-4}$	response to abiotic stimulus
		GO:0043436	1.47	$7.79 \times 10^{-4}$	oxoacid metabolic process
		GO:0006082	1.47	$7.88 \times 10^{-4}$	organic acid metabolic process
5	164	GO:0019748	3.53	$4.01 \times 10^{-5}$	secondary metabolic process
		GO:0010467	-2.44	$8.68 \times 10^{-5}$	gene expression
		GO:0006807	-1.8	$1.09 \times 10^{-4}$	nitrogen compound metabolic process
		GO:0055114	1.33	$1.68 \times 10^{-4}$	oxidation–reduction process
		GO:0006139	-1.8	$5.42 \times 10^{-4}$	nucleobase-containing compound metabolic process
		GO:0009404	4.68	$6.29 \times 10^{-4}$	toxin metabolic process
		GO:0034641	-1.64	$6.33 \times 10^{-4}$	cellular nitrogen compound metabolic process
		GO:0018874	6.41	$6.46 \times 10^{-4}$	benzoate metabolic process
		GO:0016046	6.41	$6.46 \times 10^{-4}$	detection of fungus
		GO:0044710	0.78	$6.93 \times 10^{-4}$	single-organism metabolic process
		GO:0044260	-0.99	$6.96 \times 10^{-4}$	cellular macromolecule metabolic process
		GO:0009605	2.75	$7.48 \times 10^{-4}$	response to external stimulus
		GO:0009267	3.63	$8.90 \times 10^{-4}$	cellular response to starvation
		GO:0034052	6.15	$9.65 \times 10^{-4}$	positive regulation of plant-type hypersensitive response
		GO:0098543	6.15	$9.65 \times 10^{-4}$	detection of other organism
6	79	GO:0030042	6.62	$1.10 \times 10^{-5}$	actin filament depolymerization
		GO:0051261	6.48	$1.48 \times 10^{-5}$	protein depolymerization
		GO:0043624	5.33	$1.71 \times 10^{-4}$	cellular protein complex disassembly
		GO:0043241	5.27	$1.93 \times 10^{-4}$	protein complex disassembly
		GO:0032984	5.27	$1.93 \times 10^{-4}$	macromolecular complex disassembly

Table 4. continued

cluster	N <sup>o</sup> of DEG	GO term	log 2 enrichment	p-value	description
		GO:0022411	5.19	$2.29 \times 10^{-4}$	cellular component disassembly
		GO:0009827	7.03	$3.03 \times 10^{-4}$	plant-type cell wall modification
		GO:0008154	4.66	$6.78 \times 10^{-4}$	actin polymerization or depolymerization
		GO:0007015	4.6	$7.57 \times 10^{-4}$	actin filament organization

<sup>a</sup>The DEGs belonging to each cluster are characterized by the same expression profile in the three RNA-seq comparison ( $A_{1/2}$  vs C;  $A_1$  vs C;  $A_1$  vs  $A_{1/2}$ ). In the table, the enriched or depleted terms related to biological process with a  $p$ -value  $>0.005$  are reported.

Table 5. GO Enrichment Analysis of the Six Clusters Identified<sup>a</sup>

cluster	GO term	log 2 enrichment	p-value	description
1	GO:0020037	2.97	$1.09 \times 10^{-7}$	heme binding
	GO:0016491	1.88	$1.31 \times 10^{-7}$	oxidoreductase activity
	GO:0046906	2.92	$1.54 \times 10^{-7}$	tetrapyrrole binding
	GO:0016684	3.57	$5.91 \times 10^{-6}$	oxidoreductase activity, acting on peroxide as acceptor
	GO:0004601	3.57	$5.91 \times 10^{-6}$	peroxidase activity
	GO:0016209	3.36	$1.55 \times 10^{-5}$	antioxidant activity
	GO:0046914	1.29	$5.58 \times 10^{-4}$	transition-metal ion binding
	GO:0005506	2.41	$8.92 \times 10^{-4}$	iron ion binding
2	GO:0016684	3.55	$9.89 \times 10^{-12}$	oxidoreductase activity, acting on peroxide as acceptor
	GO:0004601	3.55	$9.89 \times 10^{-12}$	peroxidase activity
	GO:0016209	3.34	$8.18 \times 10^{-11}$	antioxidant activity
	GO:0016491	1.62	$2.46 \times 10^{-10}$	oxidoreductase activity
	GO:0020037	2.51	$3.16 \times 10^{-9}$	heme binding
	GO:0046906	2.46	$5.33 \times 10^{-9}$	tetrapyrrole binding
	GO:0030410	6.29	$7.45 \times 10^{-9}$	nicotianamine synthase activity
	GO:0016765	3.79	$3.38 \times 10^{-7}$	transferase activity, transferring alkyl or aryl (other than methyl) groups
	GO:0003824	0.52	$2.28 \times 10^{-6}$	catalytic activity
	GO:0005102	4.48	$8.58 \times 10^{-5}$	receptor binding
	GO:0046522	7.29	$1.22 \times 10^{-4}$	S-methyl-5-thioribose kinase activity
	GO:0005515	-0.93	$1.94 \times 10^{-4}$	protein binding
	GO:0003676	-1.22	$4.63 \times 10^{-4}$	nucleic acid binding
	GO:0016491	1.31	$5.60 \times 10^{-4}$	oxidoreductase activity
GO:0005515	-1.23	$8.94 \times 10^{-4}$	protein binding	
4	GO:0004553	2.15	$1.99 \times 10^{-5}$	hydrolase activity, hydrolyzing O-glycosyl compounds
	GO:0016798	2	$6.18 \times 10^{-5}$	hydrolase activity, acting on glycosyl bonds
	GO:0016872	4.88	$3.97 \times 10^{-4}$	intramolecular lyase activity
	GO:0008061	4.51	$8.73 \times 10^{-4}$	chitin binding
5	GO:0020037	2.52	$4.47 \times 10^{-7}$	heme binding
	GO:0046906	2.47	$6.55 \times 10^{-7}$	tetrapyrrole binding
	GO:0016491	1.45	$4.67 \times 10^{-6}$	oxidoreductase activity
	GO:0003824	0.54	$1.73 \times 10^{-5}$	catalytic activity
	GO:0005506	2.25	$1.27 \times 10^{-4}$	iron ion binding
	GO:0010279	6.74	$3.89 \times 10^{-4}$	indole-3-acetic acid amido synthetase activity
	GO:0003676	-1.54	$5.26 \times 10^{-4}$	nucleic acid binding
	GO:0052627	6.41	$6.46 \times 10^{-4}$	vanillate amino acid synthetase activity
	GO:0052628	6.41	$6.46 \times 10^{-4}$	4-hydroxybenzoate amino acid synthetase activity
	GO:0052625	6.41	$6.46 \times 10^{-4}$	4-aminobenzoate amino acid synthetase activity
	GO:0052626	6.41	$6.46 \times 10^{-4}$	benzoate amino acid synthetase activity
	GO:0016684	2.68	$9.77 \times 10^{-4}$	oxidoreductase activity, acting on peroxide as acceptor
GO:0004601	2.68	$9.77 \times 10^{-4}$	peroxidase activity	
6	GO:0003779	4.73	$5.81 \times 10^{-4}$	actin binding

<sup>a</sup>The DEGs belonging to each cluster are characterized by the same expression profile in the three RNA-seq comparison ( $A_{1/2}$  vs C;  $A_1$  vs C;  $A_1$  vs  $A_{1/2}$ ). In the table, the enriched or depleted terms related to molecular function with a  $p$ -value  $>0.005$  are reported.

kinases (BAK1), involved in brassinosteroid (BR) signal transduction (Supporting Information S7). The half-APR dose mainly upregulates the expression of BAK1 transcripts, while the full-dose ( $A_1$ ) resulted in both induction or repression of the BR-related gene transcription. The great presence of BR-related genes among the DEGs suggests a relevant role of this hormone in the plant response to APR treatments. Besides BR-related

proteins, also auxin-related proteins (4), abscisic acid-related proteins (8), jasmonated induced proteins (3), and strigolactones biosynthesis genes (3) were identified.

## DISCUSSION

Bioestimulants contribute to sustainable, high-output, low-input crop productions.<sup>38–40</sup> Despite the fact that the use of

biostimulants is constantly increasing in modern agricultural systems, their mode of action is still poorly studied. With respect to these considerations, a RNA-seq-based analysis was conducted on maize roots to measure the effect of APR on root transcriptome. To our knowledge, this is one of the first pieces of experimental evidence for the mechanism behind the function of a biostimulant in maize.<sup>32</sup>

As can be seen from biomass analysis, APR treatments stimulate the development of a greater root system. Roots are the interface between plant and soil. By both sensing environmental cues and rearranging their architecture roots, plants adapt their development to exogenous factors, which contributes to overcoming various types of stresses. Increases in root length and number are translated to a higher uptake of water and nutrients from the soil, possibly leading to higher growth rate and/or improved tolerance to stress. Mechanisms driving these architectural adjustments are complex and involve numerous signaling events.

Overproduction of reactive oxygen species (ROS) in plant cells is caused by a wide range of both metabolic events and environmental conditions. ROS are highly toxic and ultimately result in cellular damage and death.<sup>39</sup> On the other hand, ROS also act as signals for the activation of developmental and stress response pathways.<sup>41</sup> Plants have settled an efficient enzymatic and nonenzymatic antioxidant system to protect themselves against oxidative damage and to finely modulate the ROS levels for signal transduction.<sup>42</sup> At the molecular level, APR was demonstrated to regulate the transcription of a set of genes involved in ROS homeostasis, including peroxidases, laccases, glutathione S-transferase, and glutathione peroxidase, thus likely enhancing the detoxification capacity, but the transcription of genes involved in ROS generation was not affected. These results suggest that APR could mimic in planta the same pattern of responses linked to oxidative stress, likely improving the constitutive tolerance to unexpected further stresses. Moreover, an effect of APR on the expression levels of brassinosteroid-related genes was observed. BR are ubiquitous plant steroid hormones that control both plant development and tolerance to a variety of abiotic stresses by finely modulating the antioxidant defense system.<sup>43,44</sup>

Remarkably, the transcription of nine receptor-associated kinases (BAK1) was differentially regulated by APR. The membrane-based receptor-like kinase BAK1 has been reported to contribute to a variety of signaling responses to exogenous and endogenous cues by interacting with several other membrane-based receptors.<sup>45</sup> BAK1 is a positive regulator of plant growth by its association with the plant hormone receptor BRI1 and modulates pathways involved in resistance to pathogen infection and herbivore attack by interacting with the pathogen-associated molecular pattern (PAMP) receptors.<sup>46</sup> The slight induction of the antioxidant response in APR-treated plants could therefore be mediated also by the modulation of BR signaling through the regulation of BAK1 expression. Moreover, RNA-seq analyses revealed that the highest APR concentration induces the transcription of several nitrate transporters belonging to the high affinity system, likely improving the efficiency of acquisition of nitrate.

The nicotianamine synthase (NAS) enzymes catalyze the formation of nicotianamine (NA), a nonproteinogenic amino acid involved in iron transport and homeostasis.<sup>47,48</sup> Other studies inferred that NAS enzymes are also required for proper response to cadmium supply.<sup>49–51</sup> The maize NAS gene family is composed by nine members.<sup>52</sup> Both concentrations of APR

triggered an increase in transcription for five NAS. On the basis of these preliminary results, APR may represent an environmentally friendly substitute for iron chelates and could be useful in partly relieving the deleterious effects of Cd.

Previous studies have demonstrated that transcription factors could mediate plant response to biostimulants by modulating gene expression.<sup>53</sup> In the present study, 35 genes with a role in gene expression regulation were differentially transcribed in response to APR. They belong to different transcription factors families such as the WRKYs, the ethylene-responsive factors (ERF), the basic leucine zipper (bZIP) family, and myeloblastosis protein (MYB) family (TRANSPARENT TESTA). A recent review reported that TFs belonging to five large TF families (AP2/EREBP, MYB, WRKY, NAC, and bZIP) are involved in various abiotic stresses, and some TF genes are proposed to be engineered to improve stress tolerance in model and crop plants.<sup>54</sup> In this prospective, regulating key TF expression by treatments with biostimulants could represent an alternative to genetic engineering for improvement of abiotic stress tolerance.

Stress exposure, depending on stress intensity and the species, can result in both plant cell wall loosening and tightening by affecting cellulose, hemicellulose, and pectin biosynthesis.<sup>55,56</sup> In most tolerant species, the biosynthesis of cellulose and xyloglucan is induced upon stress.<sup>56</sup> An up-regulation of the expression of genes encoding expansin and xyloglucan endo- $\beta$ -transglucosylases/hydrolases, together with that of other cell wall proteins contributing to the strengthening of the wall, including Fasciclin-like arabinogalactan protein was observed after APR provision. These results seem to suggest that APR applications could stimulate the transcription of genes encoding enzymes involved in cell wall biosynthesis and remodelling, thus priming root cells to prevent cell wall degradation and maintain cell wall extensibility upon stress conditions.

Besides this, APR seems to negatively regulate the expression of a set of genes involved in actin and microtubule polymerization or depolymerization. Microtubules act as sensors and integrators for stimuli such as mechanic load and gravity but also osmotic stress, cold, and pathogen attack.<sup>57</sup> Moreover, recently, microtubules were proposed to act as decoders of stress signals, including reactive oxygen species, calcium, or jasmonate. These preliminary results support the idea that APR could interact with the stress signaling pathway also by modulating cytoskeleton dynamic.

Globally, results herein obtained defined a complex transcriptomic signature for APR. Classification analyses clearly linked gene expression regulation to physiological, metabolic, and signaling pathways, playing key roles in stress response and possibly leading to improvement of stress tolerance to adverse environmental conditions. All together, these findings suggest that APR could activate tolerance pathways by mimicking the plant responses to environmental stresses, thus priming them against unfavorable conditions against possible stresses. In the future, testing the effectiveness of APR treatments in nonoptimal environments is crucial to assess the actual role of the specific candidate genes identified with this untargeted approach as crucial regulators of biostimulant activity.

## ■ ASSOCIATED CONTENT

### 📄 Supporting Information

The Supporting Information is available free of charge on the ACS Publications website at DOI: 10.1021/acs.jafc.7b03069.

Figure S1: Dried-weight analysis; Figure S2–S7: heat maps representing the expression profiles of DEGs belonging to the biological processes involved in the response to APR; Figure S8–S9: representation of biosynthesis of secondary metabolites of *Zea mays* L. (KEGG pathways) (PDF)

Table S1: List of the DEGs identified in the comparison A<sub>1</sub> vs C, A<sub>1/2</sub> vs C, and A<sub>1</sub> vs A<sub>1/2</sub> with their RNA-seq values (XLSX)

## AUTHOR INFORMATION

### Corresponding Author

\*E-mail: sara.trevisan@unipd.it.

### ORCID

Sara Trevisan: 0000-0001-8317-9621

### Notes

The authors declare no competing financial interest.

## ACKNOWLEDGMENTS

This work has been supported by ILSA S.p.A. S.T. was financed by a grant from ILSA S.p.A. We also thank Professor Bargelloni (BCA department, Padua University) for Bioanalyser facilities.

## REFERENCES

- Izumi, T.; Luo, J. J.; Challinor, A. J.; Sakurai, G.; Yokozawa, M.; Sakuma, H.; Brown, M. E.; Yamagata, T. Prediction of seasonal climate-induced variations in global food production. *Nat. Clim. Change* **2013**, *3*, 904–908.
- Rosenzweig, C.; Elliott, J.; Deryng, D.; Ruane, A. C.; Müller, C.; Arneth, A.; Boote, K. J.; Folberth, C.; Glotter, M.; Khabarov, N.; Neumann, K.; Piontek, F.; Pugh, T. A.; Schmid, E.; Stehfest, E.; Yang, H.; Jones, J. W. Assessing agricultural risks of climate change in the 21st century in a global gridded crop model intercomparison. *Proc. Natl. Acad. Sci. U. S. A.* **2014**, *111*, 3268–3273.
- Tilman, D.; Cassman, K. G.; Matson, P. A.; Naylor, R.; Polasky, S. Agricultural sustainability and intensive production practices. *Nature* **2002**, *418*, 671–677.
- Pretty, J.; Bharucha, Z. P. Sustainable intensification in agricultural systems. *Ann. Bot.* **2014**, *114*, 1571–1596.
- Anderson, J. A.; Gipmans, M.; Hurst, S.; Layton, R.; Nehra, N.; Pickett, J.; Shah, D. M.; Souza, T. L. P. O.; Tripathi, L. Emerging Agricultural Biotechnologies for Sustainable Agriculture and Food Security. *J. Agric. Food Chem.* **2016**, *64*, 383–393.
- Yakhin, O. I.; Lubyantsev, A. A.; Yakhin, I. A.; Brown, P. H. Biostimulants in Plant Science: A Global Perspective. *Front. Plant Sci.* **2017**, *7*, 2049.
- EBIC (2011a). Economic Overview of the Biostimulants Sector in Europe. <http://www.biostimulants.eu/> (accessed September 27, 2017).
- EBIC (2013). Economic Overview of the Biostimulants Sector in Europe. <http://www.biostimulants.eu/> (accessed September 27, 2017).
- Traon, D.; Amat, L.; Zotz, F.; du Jardin, P. A Legal Framework for Plant Biostimulants and Agronomic Fertiliser Additives in the EU. Report to the European Commission. *DG Enterprise & Industry, Arcadia International* **2014**, 115.
- Du Jardin, P. The Science of Plant Biostimulants - A Bibliographic Analysis. *Ad hoc Study Report*; European Commission: Brussels, 2012.
- Colla, G.; Roupael, Y.; Di Mattia, E.; El-Nakhel, C.; Cardarelli, M. Co-inoculation of *Glomus intraradices* and *Trichoderma atroviride* acts as a biostimulant to promote growth, yield and nutrient uptake of vegetable crops. *J. Sci. Food Agric.* **2015**, *95*, 1706–1715.
- Calvo, P.; Nelson, L.; Kloepper, J. W. Agriculture uses of plant biostimulants. *Plant Soil* **2014**, *383*, 3–41.
- Kunicki, E.; Grabowska, A.; Sękara, A.; Wojciechowska, R. The effect of cultivar type, time of cultivation, and biostimulant treatment on the yield of spinach (*Spinacia oleracea* L.). *Folia Horti* **2010**, *22*, 9–13.
- Lisiecka, J.; Knaflewski, M.; Spizewski, T.; Fraszczak, B.; Kaluzewicz, A.; Krzesinski, W. The effect of animal protein hydrolysate on quantity and quality of strawberry daughter plants cv. 'Elsanta'. *Acta Sci. Polym. Hortorum Cultus* **2011**, *10*, 31–40.
- Paradikovic, N.; Vinkovic, T.; Vrcek, I. V.; Zuntar, I.; Bojic, M.; Medic-Saric, M. Effect of natural biostimulants on yield and nutritional quality: an example of sweet yellow pepper (*Capsicum annuum* L.) plants. *J. Sci. Food Agric.* **2011**, *91*, 2146–2152.
- Colla, G.; Svecova, E.; Roupael, Y.; Cardarelli, M.; Reynaud, H.; Canaguier, R.; Planques, B. Effectiveness of a plant-derived protein Hydrolysate to improve crop performances under different growing conditions. *Acta Horti.* **2013**, *1009*, 175–180.
- Saa, S.; Olivos-Del Rio, A.; Castro, S.; Brown, P. H. Foliar application of microbial and plant based biostimulants increases growth and potassium uptake in almond (*Prunus dulcis* Mill. D. A. Webb). *Front. Plant Sci.* **2015**, *6*, 87.
- García-Martínez, A. M.; Tejada, M.; Díaz, A.; Bautista, J. D.; Rodríguez, B.; Parrado, J. Enzymatic production of an organic soil biostimulant from wheat-condensed distiller solubles: Effects on soil biochemistry and biodiversity. *Process Biochem.* **2010**, *45*, 1127–1133.
- Colla, G.; Roupael, Y.; Canaguier, R.; Svecova, E.; Cardarelli, M. Biostimulant action of a plant-derived protein hydrolysate produced through enzymatic hydrolysis. *Front. Plant Sci.* **2014**, *5*, 448.
- Lucini, L.; Roupael, Y.; Cardarelli, M.; Canaguier, R.; Kumar, P.; Colla, G. The effect of a plant-derived biostimulant on metabolic profiling and crop performance of lettuce grown under saline conditions. *Sci. Horti.* **2015**, *182*, 124–133.
- Ambigaipalan, P.; Shahidi, F. Antioxidant Potential of Date (*Phoenix dactylifera* L.) Seed Protein Hydrolysates and Carnosine in Food and Biological Systems. *J. Agric. Food Chem.* **2015**, *63*, 864–871.
- Schiavon, M.; Ertani, A.; Nardi, S. Effects of an alfalfa protein hydrolysate on the gene expression and activity of enzymes of the tricarboxylic acid (TCA) Cycle and nitrogen metabolism in *Zea mays* L. *J. Agric. Food Chem.* **2008**, *56*, 11800–11808.
- Ertani, A.; Cavani, L.; Pizzeghello, D.; Brandellero, E.; Altissimo, A.; Ciavatta, C.; Nardi, S. Biostimulant activity of two protein hydrolysates in the growth and nitrogen metabolism of maize seedlings. *J. Plant Nutr. Soil Sci.* **2009**, *172*, 237–244.
- Matsumiya, Y.; Kubo, M. Soybean peptide: novel plant growth promoting peptide from soybean. In *Soybean and Nutrition*; El-Shemy, H., Ed.; InTech Europe Publisher: Rijeka, Croatia, 2011; pp 215–230.
- Botta, A. Enhancing plant tolerance to temperature stress with amino acids: an approach to their mode of action. *Acta Horti.* **2013**, *1009*, 29–35.
- Cerdán, J.; Sanchez-Sanchez, A.; Jorda, J. D.; Juarez, M.; Sanchez-Andreu, J. Effect of commercial amino acids on iron nutrition of tomato plants grown under lime-induced iron deficiency. *J. Plant Nutr. Soil Sci.* **2013**, *176*, 859–866.
- Petrozza, A.; Santaniello, A.; Summerer, S.; Di Tommaso, G.; Di Tommaso, D.; Paparelli, E.; Piaggese, A.; Perata, P.; Cellini, F. Physiological responses to Megafol® treatments in tomato plants under drought stress: a phenomic and molecular approach. *Sci. Horti.* **2014**, *174*, 185–192.
- Visconti, F.; De Paz, J. M.; Bonet, L.; Jordà, M.; Quiñones, A.; Intrigliolo, D. S. Effects of a commercial calcium protein hydrolysate on the salt tolerance of *Diospyros kaki* L. cv. "Rojo Brillante" grafted on *Diospyros lotus* L. *Sci. Horti.* **2015**, *185*, 129–138.
- Nair, P.; Kandasamy, S.; Zhang, J.; Ji, X.; Kirby, C.; Benkel, B.; Hodges, M. D.; Critchley, A. T.; Hiltz, D.; Prithiviraj, B. Transcriptional and metabolomic analysis of *Ascophyllum nodosum* mediated freezing tolerance in *Arabidopsis thaliana*. *BMC Genomics* **2012**, *13*, 643–665.
- Povero, G.; Loreti, E.; Pucciariello, C.; Santaniello, A.; Di Tommaso, D.; Di Tommaso, G.; Kapetis, D.; Zolezzi, F.; Piaggese, A.; Perata, P. Transcript profiling of chitosan-treated *Arabidopsis* seedlings. *J. Plant Res.* **2011**, *124*, 619–629.
- Goñi, O.; Fort, A.; Quille, P.; McKeown, P. C.; Spillane, C.; O'Connell, S. Comparative Transcriptome Analysis of Two *Ascophyllum nodosum* Extract Biostimulants: Same Seaweed but Different. *J. Agric. Food Chem.* **2016**, *64*, 2980–2989.

- (32) Santi, C.; Zamboni, A.; Varanini, Z.; Pandolfini, T. Growth Stimulatory Effects and Genome-Wide Transcriptional Changes Produced by Protein Hydrolysates in Maize Seedlings. *Front. Plant Sci.* **2017**, *8*, 433.
- (33) Vezzi, F.; Del Fabbro, C.; Tomescu, A. I.; Policriti, A. rNA: a fast and accurate short reads numerical aligner. *Bioinformatics* **2012**, *28*, 123–124.
- (34) Trapnell, C.; Roberts, A.; Goff, L.; Pertea, G.; Kim, D.; Kelley, D. R.; Pimentel, H.; Salzberg, S. L.; Rinn, J. L.; Pachter, L. Differential gene and transcript expression analysis of RNA-seq experiments with TopHat and Cufflinks. *Nat. Protoc.* **2012**, *7*, 562–578.
- (35) Schnable, P. S.; Ware, D.; Fulton, R. S.; et al. The B73 maize genome: Complexity, diversity, and dynamics. *Science* **2009**, *326*, 1112–1115.
- (36) Vandepoele, K.; Van Bel, M.; Richard, G.; Van Landeghem, S.; Verhelst, B.; Moreau, H.; Van de Peer, Y.; Grimsley, N.; Piganeau, G. pico-PLAZA, a genome database of microbial photosynthetic eukaryotes. *Environ. Microbiol.* **2013**, *15*, 2147–2153.
- (37) Proost, S.; Van Bel, M.; Vaneechoutte, D.; Van de Peer, Y.; Inzé, D.; Mueller-Roeber, B.; Vandepoele, K. PLAZA 3.0: an access point for plant comparative genomics. *Nucleic Acids Res.* **2015**, *43*, D974–81.
- (38) Povero, G.; Mejia, J. F.; Di Tommaso, D.; Piaggese, A.; Warrior, P. A Systematic Approach to Discover and Characterize Natural Plant Biostimulants. *Front. Plant Sci.* **2016**, *7*, 435.
- (39) García-Martínez, A. M.; Tejada, M.; Díaz, A. I.; Rodríguez-Morgado, B.; Bautista, J.; Parrado, J. Enzymatic Vegetable Organic Extracts as Soil Biochemical Biostimulants and Atrazine Extenders. *J. Agric. Food Chem.* **2010**, *58*, 9697–9704.
- (40) Gill, S. S.; Tuteja, N. Reactive oxygen species and antioxidant machinery in abiotic stress tolerance in crop plants. *Plant Physiol. Biochem.* **2010**, *48*, 909–930.
- (41) Baxter, A.; Mittler, R.; Suzuki, N. ROS as key players in plant stress signalling. *J. Exp. Bot.* **2014**, *65*, 1229–1240.
- (42) You, J.; Chan, Z. ROS Regulation During Abiotic Stress Responses in Crop Plants. *Front. Plant Sci.* **2015**, *6*, 1092.
- (43) Krishna, P. Brassinosteroid-mediated stress responses. *J. Plant Growth Regul.* **2003**, *22*, 289–297.
- (44) Kagale, S.; Divi, U. K.; Krochko, J. E.; Keller, W. A.; Krishna, P. Brassinosteroid confers tolerance in *Arabidopsis thaliana* and *Brassica napus* to a range of abiotic stresses. *Planta* **2006**, *225*, 353–364.
- (45) Klauser, D.; Flury, P.; Boller, T.; Merker, S. Looking BAK again: Is an old acquaintance of innate immunity involved in the detection of herbivores? *Plant Signaling Behav.* **2016**, *11* (11), e1252014.
- (46) Chinchilla, D.; Zipfel, C.; Robatzek, S.; Kemmerling, B.; Nürnberger, T.; Jones, J. D.; Felix, G.; Boller, T. A Flagellin-induced complex of the receptor FLS2 and BAK1 initiates plant defence. *Nature* **2007**, *448*, 497–500.
- (47) Inoue, H.; Higuchi, K.; Takahashi, M.; Nakanishi, H.; Mori, S.; Nishizawa, N. K. Three rice nicotianamine synthase genes, OsNAS1, OsNAS2, and OsNAS3 are expressed in cells involved in long-distance transport of iron and differentially regulated by iron. *Plant J.* **2003**, *36*, 366–381.
- (48) Douchkov, D.; Gryczka, C.; Stephan, U. W.; Hell, R.; Baumlein, H. Ectopic expression of nicotianamine synthase genes results in improved iron accumulation and increased nickel tolerance in transgenic tobacco. *Plant, Cell Environ.* **2005**, *28*, 365–374.
- (49) Koen, E.; Besson-Bard, A.; Duc, C.; Astier, J.; Gravot, A.; Richaud, P.; Lamotte, O.; Boucherez, J.; Gaymard, F.; Wendehenne, D. *Arabidopsis thaliana* nicotianamine synthase 4 is required for proper response to iron deficiency and to cadmium exposure. *Plant Sci.* **2013**, *209*, 1–11.
- (50) Huang, Y. Y.; Shen, C.; Chen, J. X.; He, C. T.; Zhou, Q.; Tan, X.; Yuan, J. G.; Yang, Z. Y. Comparative transcriptome analysis of two *Ipomoea aquatica* forsk. cultivars targeted to explore possible mechanism of genotype-dependent accumulation of cadmium. *J. Agric. Food Chem.* **2016**, *64*, 5241–5250.
- (51) Yue, R.; Lu, C.; Qi, J.; Han, X.; Yan, S.; Guo, S.; Liu, L.; Fu, X.; Chen, N.; Yin, H.; Chi, H.; Tie, S. Transcriptome Analysis of Cadmium-Treated Roots in Maize (*Zea mays* L.). *Front. Plant Sci.* **2016**, *7*, 1298.
- (52) Zhou, X.; Li, S.; Zhao, Q.; Liu, X.; Zhang, S.; Sun, C.; Fan, Y.; Zhang, C.; Chen, R. Genome-wide identification, classification and expression profiling of nicotianamine synthase (NAS) gene family in maize. *BMC Genomics* **2013**, *14*, 238.
- (53) Wilson, H. T.; Xu, K.; Taylor, A. G. Transcriptome Analysis of Gelatin Seed Treatment as a Biostimulant of Cucumber Plant Growth. *Sci. World J.* **2015**, *2015*, 391234.
- (54) Joshi, R.; Wani, S. H.; Singh, B.; Bohra, A.; Dar, Z. A.; Lone, A. A.; Pareek, A.; Singla-Pareek, S. L. Transcription Factors and Plants Response to Drought Stress: Current Understanding and Future Directions. *Front. Plant Sci.* **2016**, *7*, 1029.
- (55) Storch, T. T.; Finatto, T.; Bruneau, M.; Orsel-Baldwin, M.; Renou, J. P.; Rombaldi, C. V.; Quecini, V.; Laurens, F.; Girardi, C. G. Contrasting Transcriptional Programs Control Postharvest Development of Apples (*Malus x domestica* Borkh.) Submitted to Cold Storage and Ethylene Blockage. *J. Agric. Food Chem.* **2017**, *65*, 7813–7826.
- (56) Le Gall, H.; Philippe, F.; Domon, J. M.; Gillet, F.; Pelloux, J.; Rayon, C. Cell Wall Metabolism in Response to Abiotic Stress. *Plants* **2015**, *4*, 112–166.
- (57) Nick, P. Microtubules and the Tax Payer. *Protoplasma special issue. Protoplasma* **2012**, *249* (Suppl.2), S81–S94.